

## Communications to the Editor

### Carbonyl CSA Restraints from Solution NMR for Protein Structure Refinement

Rebecca S. Lipsitz and Nico Tjandra\*

Laboratory of Biophysical Chemistry  
National Heart, Lung, and Blood Institute  
National Institutes of Health, Building 50, Room 3513  
Bethesda, Maryland 20892-8013

Received August 15, 2001

Carbonyl ( $^{13}\text{C}'$ ) chemical shift anisotropy (CSA) data from NMR experiments is important for accurately analyzing relaxation data<sup>1</sup> and for obtaining local orientation parameters such as backbone dihedral angles.<sup>2</sup> The latter can complement short-range distance data in protein structure calculations. CSA measurements of individually labeled  $^{13}\text{C}'$  sites in the solid state are well documented,<sup>3</sup> yet cumbersome to extend to fully labeled proteins. In solution, molecules tumble according to Brownian motion and only isotropic chemical shifts are observed. However, recent advances have lead to the establishment of anisotropic conditions in solution using phospholipid mixtures known as bicelles or filamentous phage particles. This imparts a small degree of protein alignment while still permitting molecular tumbling. Under these conditions one-bond residual dipolar couplings and CSA values can be measured.<sup>4</sup> The CSA is defined as the chemical shift difference between the isotropic and anisotropic states. The application of  $^{31}\text{P}$  CSA data for structure refinement has recently been performed on a DNA oligonucleotide.<sup>5</sup> Here, we demonstrate with Bax, an  $\alpha$ -helical protein which is a key mediator of apoptosis cascades,<sup>6</sup> an analogous approach using  $^{13}\text{C}'$  CSA data.

The  $^{13}\text{C}'$  CSA data was taken from an HNCOC experiment<sup>7</sup> performed at 32 °C in 2 mM DTT, 20 mM Tris buffer, pH 6.0 under isotropic and anisotropic (Pf1 phage, 12 mg/mL) conditions. The  $^{13}\text{C}'$  chemical shift is the average of the two values at each of the  $^{15}\text{N}$  doublet resonances. The magnitude of the  $^{13}\text{C}'$  CSA,  $\Delta\delta$ , was taken as the difference between the  $^{13}\text{C}'$  chemical shift in the two data sets, measured in ppb. Figure 1 shows representative data for Glutamate 61.  $^{13}\text{C}'$  CSA values were typically between  $-100$  ppb and  $+100$  ppb. The error in the measurement was estimated to be 5 ppb based on the reproducibility of the data in the  $^{15}\text{N}$  doublet. Peak positions were determined by contour averaging as described previously.<sup>8</sup> Prior to being used for structure restraints, the  $^{13}\text{C}'$  CSA values were corrected by an offset value of 43 ppb. This was due to misreferencing of the water resonance as a result of quadrupolar splitting in the  $^2\text{H}$  lock signal caused by a subset of water molecules aligned with the phage material.<sup>9</sup> Figure 2A shows the correlation of the  $^{13}\text{C}'$  CSA values between those calculated from a previously solved solution

(1) Fischer, M. W. F.; Zeng, L.; Pang, Y.; Hu, W.; Majumdar, A.; Zunderweg, E. R. P. *J. Am. Chem. Soc.* **1997**, *119*, 12629–12642.

(2) Heise, B.; Leppert, J.; Wenschuh, H.; Ohlenschlager, O.; Gorlach, M.; Ramachandran, R. *J. Biomol. NMR* **2001**, *19*, 167–169.

(3) Gu, Z.; McDermott, A. *J. Am. Chem. Soc.* **1993**, *115*, 4282–4285.

(4) Tjandra, N.; Bax, A. *Science* **1997**, *278*, 1111–1114. Tolman, J. R.; Flanagan, J. M.; Kennedy, M. A.; Prestegard, J. H. *Proc. Natl. Acad. Sci. U.S.A.* **1995**, *92*, 9279–9283.

(5) Wu, Z.; Tjandra, A.; Bax, A. *J. Am. Chem. Soc.* **2001**, *123*, 3617–3618.

(6) Suzuki, M.; Youle, R. J.; Tjandra, N. *Cell* **2000**, *103*, 645–654. Adams, J. M.; Cory, S. *Science* **1998**, *281*, 1322–1326.

(7) de Alba, E.; Suzuki, M.; Tjandra, N. *J. Biomol. NMR* **2001**, *19*, 63–67.

(8) Wang, A. C.; Bax, A. *J. Am. Chem. Soc.* **1996**, *118*, 2483–2494.

(9) Hansen, M. R.; Mueller, L.; Pardi, A. *Nat. Struct. Biol.* **1998**, *5*, 1065–1074.

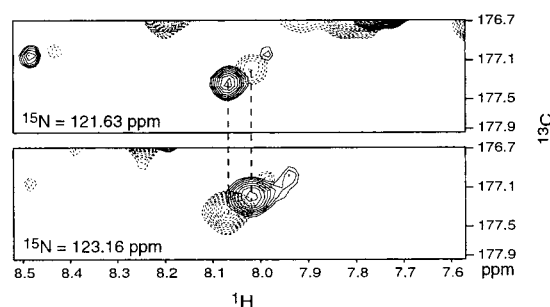


**Figure 1.** Data from the HNCOC experiment for residue Glu 61. The two antiphase  $^{15}\text{N}$  doublet components are shown. Positive and negative resonances are shown in solid and dotted lines, respectively. The isotropic and anisotropic resonances are at 8.07 and 8.02 ppm, respectively. The  $^{13}\text{C}'$  chemical shift is taken as the average value of the two doublet resonance.

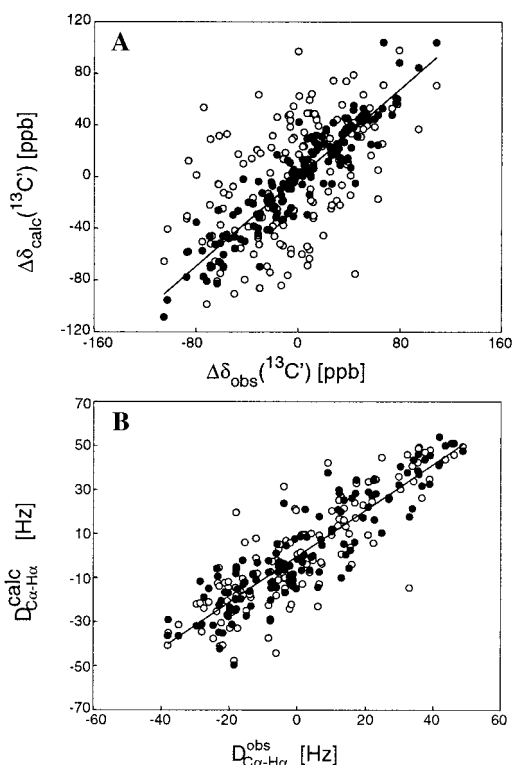


**Figure 2.** (A) Correlation between the calculated  $^{13}\text{C}'$  CSA values based on the unrefined structure of Bax ( $\circ$ ,  $R = 0.52$ ) and the  $^{13}\text{C}'$  CSA-refined structure ( $\bullet$ ,  $R = 0.92$ ) with the observed  $^{13}\text{C}'$  CSA values. (B) Correlation between the  $\text{C}\alpha\text{--H}\alpha$  one-bond residual dipolar couplings ( $D_{\text{CH}}$ ) calculated from the structure and the observed values for structures calculated without the  $^{13}\text{C}'$  CSA restraints ( $\circ$ ,  $R = 0.85$ ) and with the  $^{13}\text{C}'$  CSA restraints ( $\bullet$ ,  $R = 0.90$ ).

structure of Bax and the offset-corrected CSA values taken from experimental data. Deviation from an exact correlation reflects the quality of the starting structure.

The CSA is related to the orientation of the  $^{13}\text{C}'$  shielding tensor as follows:

$$\Delta\delta = \sum_{i=x,y,z} \sum_{j=x,y,z} A_{ij} \cos^2 \theta_{ij} \delta_{ii} \quad (1)$$

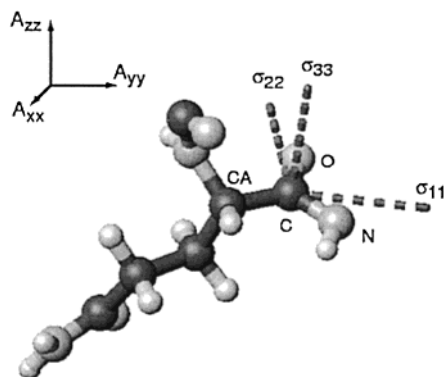


**Figure 3.** Orientation of the  $^{13}\text{C}'$  chemical shielding tensor in a molecular frame where  $A_{xx}$ ,  $A_{yy}$ , and  $A_{zz}$  are the components of the molecular alignment tensor.

where  $\theta_{ij}$  is the angle between the  $A_{ij}$  principal axis of the diagonalized traceless alignment tensor and the  $\delta_{ij}$  principal axis of the traceless CSA tensor.<sup>10</sup> The principal components of the  $^{13}\text{C}'$  alignment tensor are illustrated in Figure 3. We follow the commonly used convention  $\sigma_{33} \geq \sigma_{22} \geq \sigma_{11}$ . The magnitude and orientation of  $A_{ij}$  were determined using a least-squares fit between the one-bond  $^1\text{H}$ – $^{15}\text{N}$  residual dipolar coupling data and those calculated from the structure.<sup>11</sup> Since  $A_{ij}$  differs for each type of anisotropic sample conditions, the  $\Delta\delta$  values were measured on the same sample used for measuring the dipolar coupling data. The  $^{13}\text{C}'$  CSA tensor values used were  $\sigma_{11} = -71.2$ ,  $\sigma_{22} = -23.3$ , and  $\sigma_{33} = 94.5$ , as previously determined.<sup>12</sup>

To use the  $^{13}\text{C}'$  CSA values for structure refinement, a subroutine was added to the XPLOR 3.84 program<sup>13</sup> such that the CSA values are used as restraints which satisfy the energy function:

$$E_{\text{CSA}} = k_{\text{CSA}} (\Delta\delta_{\text{obs}} - \Delta\delta_{\text{calc}})^2 \quad (2)$$

The force constant,  $k_{\text{CSA}}$ , was adjusted to 0.003 kcal/ppb<sup>2</sup> for the rms between  $\Delta\delta_{\text{obs}}$  and  $\Delta\delta_{\text{calc}}$  to be equal to 16 ppb to take into account the measurement error and the goodness of the fit of the  $^{13}\text{C}'$  CSA tensor.<sup>11</sup> Inclusion of the  $^{13}\text{C}'$  CSA restraints caused no significant increase in the non-CSA energy terms.

One method to determine the contribution of including the  $^{13}\text{C}'$  CSA data in improving the solution structure is to monitor the change in the quality of the ensemble of structures. The quality is reflected in the improved correlation between the calculated and observed values of a given structural restraint that is omitted from the structure calculations. Here, we have selected the  $\text{C}\alpha$ – $\text{H}\alpha$  residual dipolar couplings ( $D_{\text{CH}}$ ) for this purpose. The rmsd between the measured and calculated  $D_{\text{CH}}$  has been determined for both the ensemble of structures without the CSA restraints and the ensemble of structures with the CSA restraints. Figure 2B shows the correlation between  $D_{\text{CH}}(\text{calc})$  and  $D_{\text{CH}}(\text{obs})$  without the  $^{13}\text{C}'$  CSA restraints (○) and with the CSA restraints (●). For

(10) Cornilescu, G.; Marquardt, J. L.; Ottiger, M.; Bax, A. *J. Am. Chem. Soc.* **1998**, *120*, 6836–6837.

(11) Tjandra, N.; Grzesiek, S.; Bax, A. *J. Am. Chem. Soc.* **1996**, *118*, 6264–6272.

(12) Cornilescu, G.; Bax, A. *J. Am. Chem. Soc.* **2000**, *122*, 10143–10154.

(13) Brünger, A. T. *XPLOR: A System for X-ray Crystallography and NMR*, 3.1 ed.; Yale University Press: New Haven, 1993.

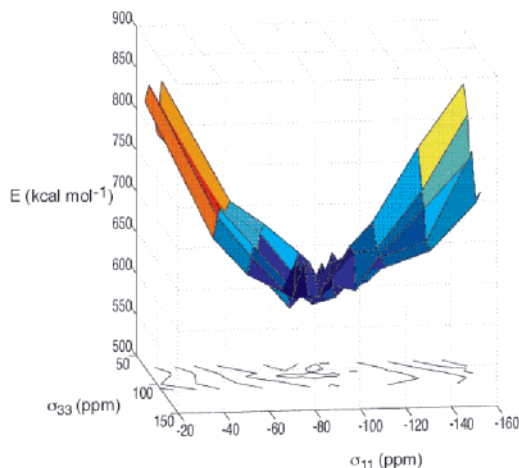


**Figure 4.** Three-dimensional plot showing the overall energy of the protein structure refined with  $^{13}\text{C}'$  CSA restraints as a function of the  $^{13}\text{C}'$  CSA tensor components  $\sigma_{11}$  and  $\sigma_{33}$ .

each of the two data sets, 30 structures were calculated, and the 10 lowest-energy structures from each set were used to determine the  $D_{\text{CH}}$  RMSD. Clearly, the quality of the structures improved by the inclusion of the  $^{13}\text{C}'$  CSA restraints. In the case of ubiquitin, when CSA restraints are included in addition to NOE restraints, the backbone pairwise rmsd from the X-ray crystallography structure is 0.6 Å, while leaving out the CSA restraints leads to a backbone pairwise rmsd of 0.7 Å. A similar effect was also observed for Bax.

For the  $^{13}\text{C}'$  CSA subroutine to be widely applicable we have taken into account the fact that the values of the  $^{13}\text{C}'$  CSA tensor elements are highly sensitive to the  $^{13}\text{C}'$  protonation state and hydrogen-bonding state.<sup>14</sup> Previous work from solid-state NMR studies demonstrates the  $\sigma_{11}$  and  $\sigma_{22}$  principal components exhibit unique values for protonated and deprotonated carbonyls<sup>15</sup> with  $\sigma_{11}$ , varying from –63 ppm (protonated) to –80 ppm (deprotonated). It is critical to understand how different CSA tensor values affect the total energy of the refined protein structure since the hydrogen-bonding state of each individual amino acid is not always well characterized. Figure 4 shows the results of a grid search where the total energy was monitored as a function of varying both  $\sigma_{11}$  and  $\sigma_{33}$  for a range of values corresponding to the protonated and deprotonated carbonyls ( $\sigma_{22}$  was changed appropriately to satisfy the definition of a traceless tensor:  $\sigma_{11} + \sigma_{22} + \sigma_{33} = 0$ ). The plot exhibits a very wide local minimum which shows similar energies for  $^{13}\text{C}'$  CSA tensor values corresponding to both protonated and deprotonated forms.

The addition of  $^{13}\text{C}'$  CSA restraints helps define the orientation of each carbonyl in the protein to a common reference frame and is a useful complement to distance restraints. The ease with which the data is acquired and incorporated into structure calculations should ensure the routine use of  $^{13}\text{C}'$  CSA data in structure calculations.

JA016854G

(14) Gu, Z.; Zambrano, R.; McDermott, A. *J. Am. Chem. Soc.* **1994**, *116*, 6368–6372.

(15) Gu, Z.; Drueckhammer, D. G.; Kurz, L.; Liu, K.; Martin, D. P.; McDermott, A. *Biochemistry* **1999**, *38*, 8022–8031.